Inducible reporter/driver lines for the Arabidopsis root with intrinsic reporting of activity state

Frank Qasim Machin, Malin Beckers, Xin Tian, Alice Fairnie, Teri Cheng, Wolf-Ruediger Scheible, Peter Doerner

TECHNICAL ADVANCE

Inducible reporter/driver lines for the Arabidopsis root with intrinsic reporting of activity state

Frank Qasim Machin[1], Malin Beckers[1], Xin Tian[1,†], Alice Fairnie[1], Teri Cheng[1], Wolf-Rüdiger Scheible[2,‡] and Peter Doerner[1,2,3,*] (iD)

[1]*Institute for Molecular Plant Science, University of Edinburgh, Edinburgh, UK,*
[2]*Max-Planck Institute of Molecular Plant Physiology, Science Park, Golm, Germany, and*
[3]*Laboratoire de Physiologie Cellulaire & Végétale, University Grenoble Alpes, CNRS, CEA, INRA, BIG-LPCV, 38000, Grenoble, France*

SUMMARY

Cell-, tissue- or organ-specific inducible expression systems are powerful tools for functional analysis of changes to the pattern, level or timing of gene expression. However, plant researchers lack standardised reagents that promote reproducibility across the community. Here, we report the development and functional testing of a Gateway-based system for quantitatively, spatially and temporally controlling inducible gene expression in Arabidopsis that overcomes several drawbacks of the legacy systems. We used this modular driver/effector system with intrinsic reporting of spatio-temporal promoter activity to generate 18 well-characterised homozygous transformed lines showing the expected expression patterns specific for the major cell types of the Arabidopsis root; seed and plasmid vectors are available through the Arabidopsis stock centre. The system's tight regulation was validated by assessing the effects of diphtheria toxin A chain expression. We assessed the utility of Production of Anthocyanin Pigment 1 (PAP1) as an encoded effector mediating cell-autonomous marks. With this shared resource of characterised reference driver lines, which can be expanded with additional promoters and the use of other fluorescent proteins, we aim to contribute towards enhancing reproducibility of qualitative and quantitative analyses.

Keywords: tissue- and cell-type-specific reporter, estradiol-inducible, reference lines, PRODUCTION OF ANTHOCYANIN PIGMENT 1 (PAP1), *Arabidopsis thaliana*, technical advance.

INTRODUCTION

Inducible gene expression systems are commonly used molecular tools to examine gene function, which remains an important challenge in the post-genomic era. These systems are used to conditionally knock-down or induce gene expression, and to investigate the short- or long-term effects of specific transgene expression when its precise control is essential for the experimental design. Many variations of such systems exist that allow for spatial and/or temporal control of the gene expression. Inducible systems are frequently used in developmental studies (Haseloff, 1999; Brand *et al.*, 2006; Marques-Bueno *et al.*, 2016; Siligato *et al.*, 2016). However, existing systems have a number of drawbacks: enhancer-trap or promoter-trap lines are in a

background now rarely used for genetic studies (e.g. C24; Goddijn *et al.*, 1993; Haseloff, 1999), thus resulting in plants with a mixed-accession lineage when introduced into commonly used mutants in the Col or L*er* backgrounds that can cause undesired side-effects (Haseloff, 1999; Laplaze *et al.*, 2005). Some systems are not restricted to specific cell types or developmental domains (Haseloff, 1999), are not inducible (Haseloff, 1999) or use the dexamethasone-inducible system GVG, which is known to have side-effects and does not show a differentiated dose–response (Kang *et al.*, 1999; Zuo *et al.*, 2000; Marques-Bueno *et al.*, 2016; Schurholz *et al.*, 2018). Some systems do not necessarily or intrinsically report successful induction, as the inclusion of a fluorescent reporter is not a mandatory feature (Siligato *et al.*, 2016), others offer few or no options for fluorescent

153

reporters (Brand *et al.*, 2006; Marques-Bueno *et al.*, 2016), utilise a more involved three-fragment recombination system (Marques-Bueno *et al.*, 2016; Siligato *et al.*, 2016), or do not provide freely accessible, specific and well-characterised transgenic lines as reference and basis for comparative studies in different laboratories (Siligato *et al.*, 2016). While the widespread use of existing expression systems attests to their utility in many situations, we identified a need for a system of standard parts that can be used for accurate and reproducible, qualitative *and* quantitative, comparison of gene expression, for example when present in different mutant backgrounds or when utilised in different laboratories. The community-wide use of such well-defined reference resources has recently been facilitated by the optimisation of CRISPR/Cas9-based methods, which make it easier to regenerate desired single or multiple hypomorphic alleles in such a standard reporter line than to introgress such alleles over several generations (Ordon *et al.*, 2017).

Several inducible systems are based on the synthetic XVE transcription factor (Zuo *et al.*, 2000; Brand *et al.*, 2006; Siligato *et al.*, 2016). The XVE factor is constructed from three modules, the bacterial transcriptional repressor *LexA* as a DNA-binding domain, the transcription-activating domain of the herpes simplex virus transcription factor VP16, and the regulatory region of the human estrogen receptor (Zuo *et al.*, 2000). This sensitive system has negligible or no background expression in Arabidopsis, and is not known to cause XVE-independent gene expression in Arabidopsis (Zuo *et al.*, 2000; Brand *et al.*, 2006; Siligato *et al.*, 2016). Plants grown in tissue culture are easy to induce with small molecules and every part of the plant can easily be exposed to estradiol, which does not move readily over long distances in the plant (Brand *et al.*, 2006). Moreover, the XVE system is dose-responsive, allowing induction to be tuned quantitatively (Zuo *et al.*, 2000). Therefore, by placement of XVE under control of tissue-, cell type- or developmental phase-specific promoters, exquisite quantitative fine-tuning of spatial and temporal gene expression can be achieved.

In the presence of estradiol, the XVE factor enters the nucleus and binds to LexA operator sequences (LexAop) placed upstream of a minimal promoter, allowing transcription of the gene of interest. Activation of gene expression mediated by XVE is not restricted to a single target, the introduction of one or more genes under control of LexAop sequences enables expression of multiple genes in parallel within the same domain.

We exploited the properties of the XVE/LexAop system to develop a set of binary vectors that permit the introduction, with Gateway® technology (https://www.thermofisher.com/uk/en/home/life-science/cloning/gateway-cloning.html), of a promoter of choice to express XVE. The desired promoter or secondary effector gene must be flanked with attL1/attL2 sequences, for which established collections exist (Xiao *et al.*, 2010). These vectors carry, in *cis*, LexAop sequences located upstream of alternatively, H2B-green fluorescent protein (GFP), H2B-yellow fluorescent protein (YFP), H2B-mKusabira Orange or H2B-mCherry fluorescent fusion proteins that function as primary effector genes to report successful induction by estradiol (Tsien, 1998; Nagai *et al.*, 2002; Karasawa *et al.*, 2004; Shaner *et al.*, 2004). Secondary effector genes are then introduced into the driver lines by crossing or by transformation. The use of a specific effector line introduced by crossing across different driver–effector line combinations provides better comparability in functional studies. To facilitate the use of common reagents and increase reproducibility across the community, we generated robustly characterised cell-type-specific driver lines for most cell types in the Arabidopsis root, which can be used as standard, modular components for gene expression and synthetic biology studies. Each of these primary lines need to be made only once and then is used as a standard part into which secondary genes are transformed. These lines have been donated to the Nottingham Arabidopsis Stock Centre.

RESULTS

A pXVE system with fluorescent reporters for modular control of localised gene expression

We developed an inducible expression system that uses two different plasmid constructs, one that acts as a Driver, which directs estradiol-inducible gene expression of a nuclear-localised fluorescent protein used to indicate successful induction and appropriate localisation in *cis*. The second plasmid construct is the Effector, that allows the expression of one or more additional genes under the control of the promoter used in the Driver line in *trans,* for example pMDC160 or pMDC221 (Brand *et al.*, 2006; Figures 1a, S1 and S16).

Four different Driver plasmid constructs were made, each carrying either eGFP (pXVG), Venus (pXVV), mKO2 (pXVK) or mCherry (pXVC), respectively (Figure S2). This facilitates their use in genetic backgrounds with pre-existing fluorescent markers or other fluorescent dyes. We tested these vectors by recombining each one with the 1947-bp promoter for AQC1 (Zhou *et al.*, 2010), which directs expression in the QC, columella stem cells and their immediate progeny (Figure 1a–d). These lines are listed in Table S2.

Reporter lines marking the major tissue types of the Arabidopsis root

The Arabidopsis primary root comprises distinct cell types, including the root cap, epidermis, cortex, endodermis and vasculature. We generated reporter lines marking the individual cell types that comprise the radial pattern of the primary root (Table S2).

The epidermis of the Arabidopsis primary root is divided into two types of cells: trichoblasts, which elongate to form

Figure 1. Driver plasmids encode tissue-specific, estradiol-inducible fluorescent reporters.

(a) Schematic representation of the inducible activator/effector XVE system. Promoter of choice recombined with vector of choice (Figures S1 and S2) by Gateway reaction is positioned upstream of the XVE synthetic transcription factor. XVE protein (hexagon) accumulation is determined by the activity domain of the promoter. Upon treatment with estradiol, the XVE protein enters the nucleus and binds to the LexAop, thus activating expression of the specific reporter and, if desired, of additional effector genes. The activity reporter (here: H2B-Venus) is localised to the nucleus, additional effectors may, but do not have to, be nuclear-localised.

(b–e) Confocal images of plant lines transformed with constructs generated by recombining the AQC1 promoter upstream of the XVE transcription factor using (b) green fluorescent protein (GFP), (c) VENUS, (d) mKusabira Orange or (e) mCherry in the pXVG, pXVV, pXVK, pXVC vectors (Figure S2), respectively. (b) Primary root meristem of the G240 line carrying proAQC1:XVE in pXVG. (c) Primary root meristem of V241 line carrying proAQC1:XVE in pXVV. (d) Primary root meristem of K242 line carrying proAQC1:XVE in pXVK. (e) Primary root meristem of C243 line carrying proAQC1:XVE in pXVC. Scale bar: 50 μm (b); 100 μm (c–e).
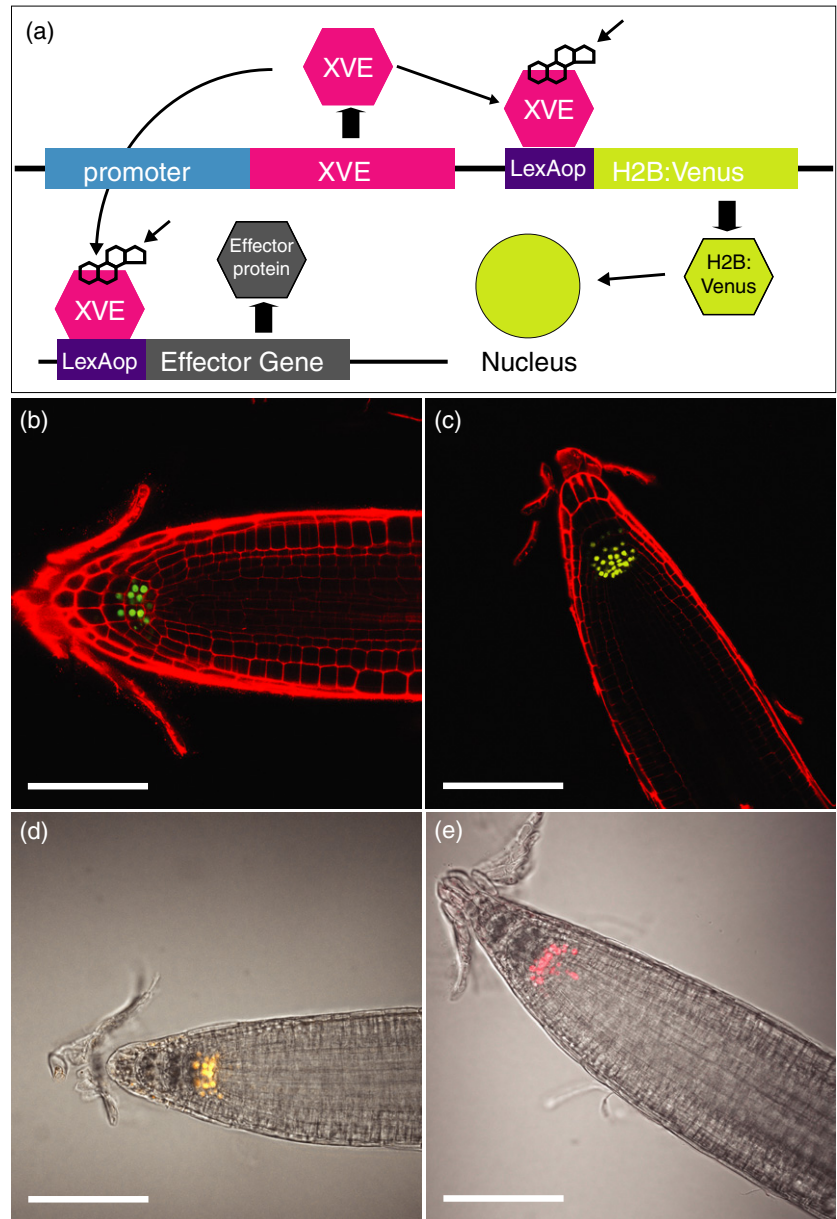
root hairs; and atrichoblasts, which do not. The atrichoblast cells are marked in a line (V101) making use of the GL2 (At1g79840) promoter. When induced by estradiol, this line shows H2B-Venus accumulation only in the atrichoblast file of the epidermis, beginning at the stem cells and continuing into the mature root (Figure 2a). The transverse section and view of the root surface show that accumulation is present only in alternating cell files of the epidermis layer and absent in the trichoblast file (Figures 2b and S3a–d). The transverse section shows that this file is located above the cell walls of single cortex cells, a trait that is necessary to pattern the atrichoblast file (Figure 2c).

Elongating trichoblast cells were marked using the SHV2 (At5g49270) promoter as this gene is required for the remodelling of the cell wall that occurs during elongation. Venus accumulation in this line (V111) is absent in the apical meristem (Figure S4d) and becomes visible starting from the transition domain, where the root hairs begin to extend from the root surface (Figures 2d and S4a,c,e). This continues into the mature root, where the labelled nuclei move into the basal region of the root hair (Figures 2e and s4b,f). The transverse section image shows that the accumulation is complementary to that of the atrichoblast line, and that the labelled cells are localised above the groove between two cortex cells (Figure 2f).
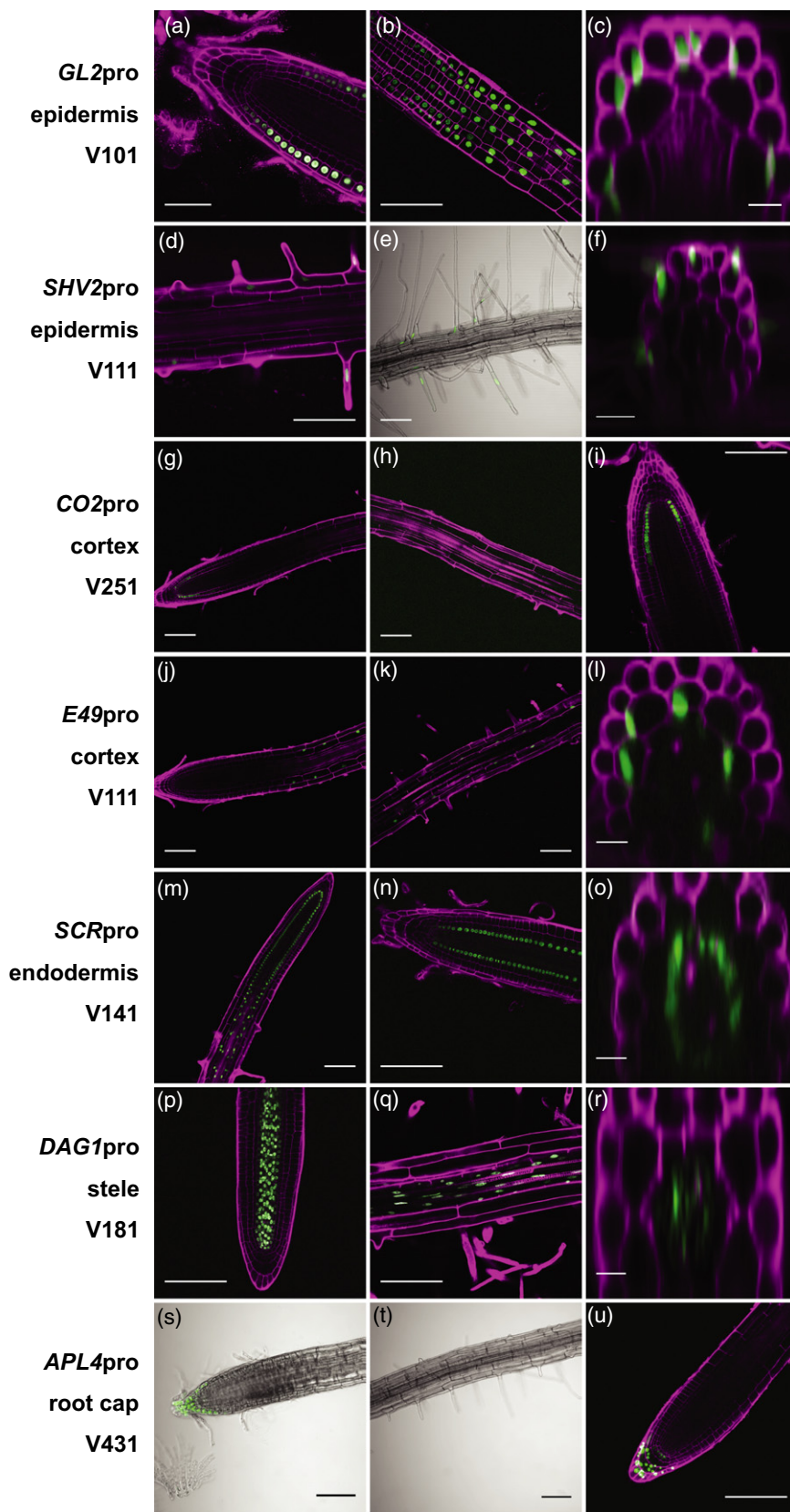
Figure 2. Driver lines for tissue-specific expression in major tissue layers of the primary root.

Unless otherwise stated, the green channel is H2B-Venus fluorescence and the magenta channel is propidium iodide (PI) staining.

(a–c) Expression in the atrichoblast cells of the epidermis. (a) Line V101 focused on the primary root meristem. Scale bar: 50 μm. (b) Transition zone of the upper epidermis of the primary root meristem of line V101. Scale bar: 100 μm. (c) Digital cross-section of the mature root of V101. Scale bar: 10 μm.

(d–f) Expression in the trichoblast cells of the epidermis. (d) Line V111 focused on the transition zone. Scale bar: 100 μm. (e) Mature root of V111, not stained with PI. Scale bar: 100 μm. (f) Digital cross-section of the mature root of V111. Scale bar: 20 μm.

(g–i) Expression in the meristematic cortex cells. (g) Primary root tip of V251. Scale bar: 100 μm. (h) Mature root of V251. Scale bar: 100 μm. (i) Primary root meristem of V251. Scale bar: 100 μm.

(j–l) Expression in the post-meristematic cortex cells. (j) Primary root tip of V121. Scale bar: 100 μm. (k) Mature root of V121. Scale bar: 100 μm. (l) Digital cross-section of mature root of V121. Scale bar: 10 μm.

(m–o) Expression in the endodermis and stem cell niche. (m) Primary root tip of V141. Scale bar: 100 μm. (n) Primary root meristem of V141. Scale bar: 100 μm. (o) Digital cross-section of mature root of V141. Scale bar: 10 μm.

(p–r) Expression in the stele. (p) Primary root meristem of V181. Scale bar: 100 μm. (q) Mature root of V181. Scale bar: 100 μm. (r) Digital cross-section of mature root of V181. Scale bar: 10 μm.

(s–u) Expression in the root cap. (s) Primary root tip of V431. Not stained with PI. Scale bar: 100 μm. (t) Mature root of V431. Not stained with PI. Scale bar: 100 μm. (u) Maximum intensity projection of a Z-stack image of primary root meristem of V431. Scale bar: 100 μm.

We did not identify a promoter sequence that directs gene expression uniformly in the entire cortex file. Therefore, two lines were made: one that expresses in the meristem cortex cells and one in the mature cortex cells. The CO2 (At1g62500) promoter sequence was used to develop a line (V251) expressing in the young cortex cells of the root apical meristem (Heidstra *et al.*, 2004). This line shows H2B-Venus accumulation in the cortical layer that begins at the stem cells and continues in the meristem region (Figures 2g,i and S5b–d). The fluorescence stops before or at the transition domain, and is not present in the mature root (Figures 2h and S5a). The mature cortex line (V121), driven by the E49 (At3g05150) promoter (Lee *et al.*, 2006), shows H2B-Venus accumulation in only the cortical layer that begins in the transition domain and continues into the mature root (Figures 2j,k and S6a–c). The fluorescence is restricted to the cortical layer, as can be seen in the transverse section (Figure 2l).

Expression in the endodermis cell layer was controlled by the SCR (At3g54220) promoter. The line transformed with this construct (V141) shows H2B-Venus accumulation in the endodermis, beginning at the stem cell niche, endodermal/cortical stem cells and continuing into the mature root (Figures 2m,n and S7a,b). This is consistent with previous observations (Helariutta *et al.*, 2000). Radially, H2B-Venus accumulation in V141 is confined to the endodermis layer, as seen in the digital cross-section (Figure 2o).

The stele line (V181) shows H2B-Venus accumulation in multiple tissues of the vascular cylinder, under the control of the DAG1 (At3g61850) promoter (described as S2 in Lee *et al.*, 2006). Fluorescence begins at the stele stem cells (Figures 2p and S8b,c) and continues into the mature root (Figures 2q and S8a), and includes H2B-Venus accumulation in the pericycle layer in the mature tissues (Figure 2r).

The root cap is a major sensory and assimilatory tissue of the Arabidopsis root that perceives external conditions, assimilates nutrients and coordinates growth responses (Tsugeki and Fedoroff, 1999; Kanno *et al.*, 2016; Su *et al.*, 2017). The APL4 (At2g21590) promoter was used to

generate a line (V431) for root cap expression (Birnbaum *et al.*, 2003). H2B-Venus fluorescence was localised to the root cap (Figure 2s) and was not seen in other parts of the primary root (Figure 2t). Venus accumulation was seen in both the columella cells as well as the lateral root cap cells (Figure 2s,u).

Reporter lines marking the pericycle

Pericycle cells comprise the outermost layer of the vasculature. They are functionally patterned by their position relative to the underlying phloem and xylem vessels, and hence are referred to as phloem pole and xylem pole pericycle cells, respectively. These are important cell types in Arabidopsis growth and development as the phloem pole pericycle cells have been implicated in regulating efflux from the phloem (Ross-Elliott *et al.*, 2017) and the xylem pole pericycle cells are the site of lateral root initiation (van Tieghem and Douliot, 1888; Esau, 1965; Steeves and Sussex, 1989; Charlton, 1991; Parizot *et al.*, 2008). We made lines marking the pericycle layer as a whole (V151), using promoter sequences of At5g09760 (Brady *et al.*, 2007) and additional lines for the phloem pole pericycle cells (V161), using promoter sequences of At2g22850 (described as S17 in Lee *et al.*, 2006); and xylem pole pericycle cells (V171), using promoter sequences of At3g29635 (Brady *et al.*, 2007), respectively (Table S1).

Fluorescent protein accumulation in the pericycle line (V151) can be seen from the beginning of the transition zone (Figures 3a and S9b,c), where the vascular tissues begin to develop, at the same time as the polar pericycle cells are specified (Pyo *et al.*, 2004; Parizot *et al.*, 2008; Yamaguchi *et al.*, 2008) and persisting through the mature root (Figures 3b and S9a,d). The transverse image shows fluorescent protein accumulate in all cells of the pericycle layer (Figure 3c).

Fluorescent protein accumulation in phloem pole pericycle nuclei (V161) can be seen from the beginning of the transition zone (Figure 3d), clustered around the developing phloem vessels can be seen most clearly when the
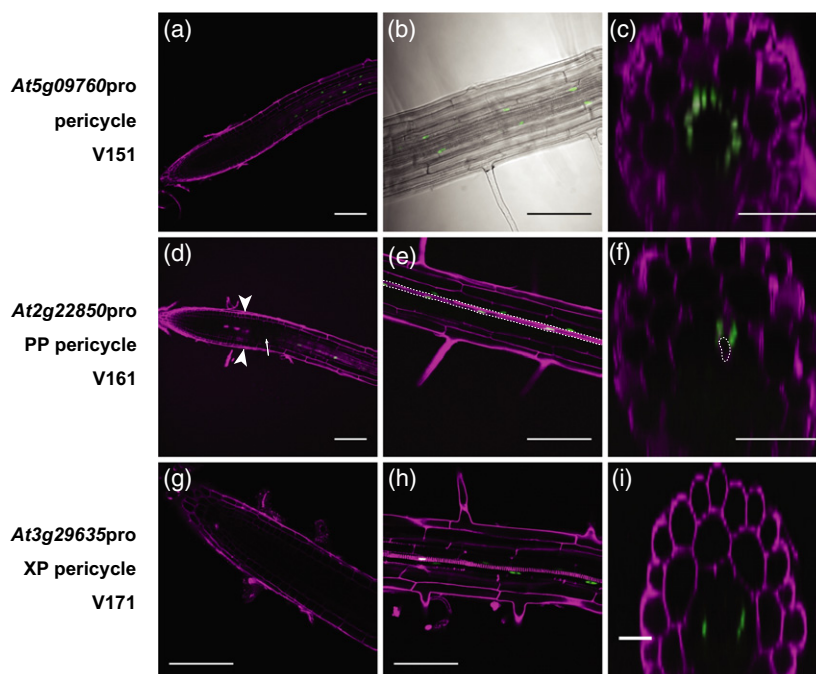
Figure 3. Driver lines for tissue-specific expression in the pericycle tissues of the primary root.
Unless otherwise stated, the green channel is H2B-Venus fluorescence and magenta is propidium iodide (PI) staining.
(a–c) Expression in pericycle cells. (a) Primary root tip of V151. Scale bar: 100 μm. (b) Mature root of V151. Not stained with PI. Scale bar: 100 μm. (c) Digital cross-section of mature root of V151. Scale bar: 50 μm.
(d–f) Expression in phloem pole pericycle cells. (d) Primary root tip of V161. Scale bar: 100 μm. Arrowheads indicate the boundary of the transition domain, the arrow indicates the first phloem pole pericycle cell with visible accumulation of fluorescent H2B-Venus. (e) Mature root of V161 stained with PI and carboxyte-traethylrhodamine (CTER). CTER staining of the phloem is highlighted by the white dashed lines. Scale bar: 100 μm. (f) Digital cross-section of mature root of V161 stained with CTER. CTER staining of the phloem is highlighted by the white dashed lines. Scale bar: 50 μm.
(g–i) Expression in xylem pole pericycle cells. (g) Primary root tip of V171. Scale bar: 100 μm. (h) Mature root of V171. Scale bar: 100 μm. (i) Digital cross-section of mature root of V171. Scale bar: 10 μm.

phloem is labelled with CTER (Figure 3e), a phloem-mobile fluorescent dye (Knoblauch *et al.*, 2015). After loading cotyledons with CTER, it is translocated via the phloem to the primary root tip, staining only the phloem vessels with a bright fluorescent signal. This is necessary to distinguish the location of cells in the centre of the root, as propidium iodide is not able to diffuse past the intact Casparian strip, which is present in differentiated endodermis cells. Loading the leaves with CTER results in the appearance of bright fluorescence in the phloem at the centre of the root (Figure 3e). The phloem pole pericycle nuclei marked with H2B-Venus fluorescent protein are situated adjacent to the phloem vessels, as seen in the transverse section image of a root stained with CTER (Figure 3f).

The H2B-Venus fluorescent marker protein reporting the activity of the xylem pole pericycle-specific promoter begins to accumulate in nuclei clustered around xylem vessels (V171), which fluoresce with propidium iodide staining in a characteristic pattern of rings, indicating maturing xylem vessels (Figure 3h). This promoter is not yet active in the primary root apical meristem (Figure 3g). Fluorescent protein accumulation can also be seen in the centre of the transverse section, with the fluorescent nuclei

of the xylem pole pericycle cells positioned adjacent to the xylem vessels (Figure 3h).

Reporter lines marking different vascular tissues

The vasculature of the Arabidopsis primary root is patterned both radially and longitudinally, with cells developing and differentiating in the longitudinal axis of the root and, during this developmental process, the opposing poles of the xylem and phloem are organised radially. Therefore, we made marker lines specific for the vascular cell types themselves and also for their progenitor cells in the apical meristem (Table S2).

Mature xylem vessels are dead, so it was not possible to generate a marker line. In its place, we made use of a promoter that is expressed in the developing xylem cells. The mature phloem tissues, in contrast, comprise living cells and so can be marked with a reporter line. Two separate lines were made for the phloem, one specific for the protophloem cells and another for the companion cells of the mature phloem.

The protophloem cells are marked by using the promoter sequences of At2g18380 (described as S32 in Lee *et al.*, 2006) in the V201 line. H2B-Venus accumulation in
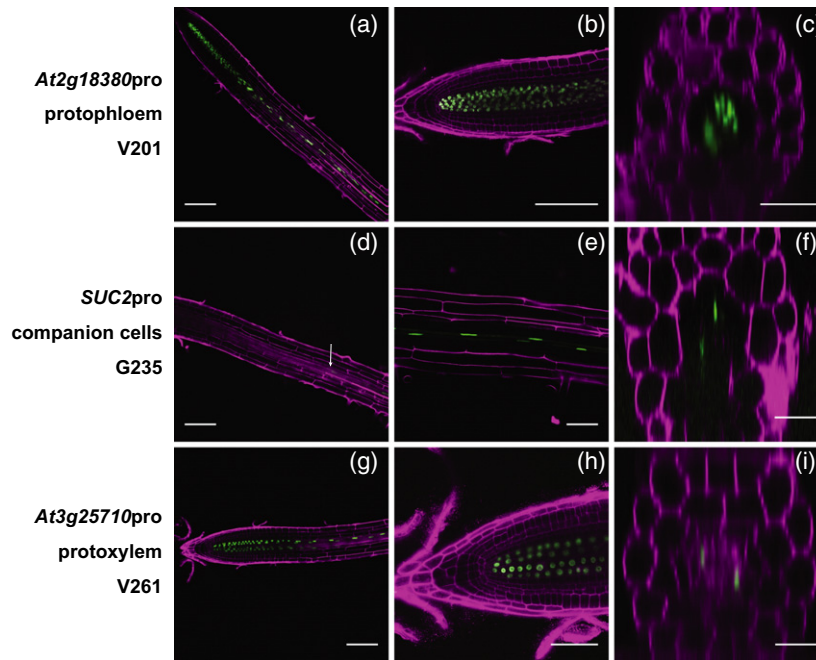
Figure 4. Driver lines for tissue-specific expression in the vascular tissues of the primary root.
Unless otherwise stated, the green channel is H2B-Venus fluorescence and magenta is propidium iodide (PI) staining.
(a–c) Expression in protophloem cells. (a) Primary root tip of V201. Scale bar: 100 μm. (b) Primary root meristem of V201. Scale bar: 100 μm. (c) Digital cross-section of mature root of V201. Scale bar: 50 μm.
(d–f) Expression in companion cells. (d) Transition zone of primary root of G235. Green fluorescence is H2B-green fluorescent protein (GFP), the arrow marks a fluorescent nucleus. Scale bar: 100 μm. (e) Mature root of G235. Green fluorescence is H2B-GFP. Scale bar: 50 μm. (f) Digital cross-section of mature root of G235. Green fluorescence is H2B-GFP. Scale bar: 25 μm.
(g–i) Expression in protoxylem cells. (g) Primary root tip of V261. Scale bar: 100 μm. (h) Primary root meristem of V261. Scale bar: 50 μm. (i) Digital cross-section of mature root of V261. Scale bar: 25 μm.

this line begins in the nuclei of the vascular initial cells and is strong in the meristem (Figures 4a,b and S10a–d). The number of cells accumulating H2B-Venus is reduced in the transition domain as cells begin to expand and the phloem develops, and then accumulates more strongly in phloem and phloem-associated cells of the mature root (Figures 4a,c and S11a,c).

The G235 line marking the companion cells of the phloem driven by the SUC2 (At1g22710) promoter shows that H2B-GFP is absent in the meristem (Figure S12c) and beginning to accumulate at the transition domain where the phloem matures (Figure 4d), and continues through the length of the phloem (Figures 4e and S12b,d). A digital cross-section reveals expression confined to the companion cells (Figure 4f). In CTER-treated plants, the fluorescence is localised in the nuclei of cells next to the phloem sieve elements that transport CTER (Figure S12a).

The developing xylem cells are marked by using promoter sequences of At3g25710 (described as S4 in Lee *et al.*, 2006, line V261). Nuclei accumulating H2B-Venus are observed in the vascular stem cells and in the xylem vessels as they develop (Figures 4g,h, S11b,d and S13a–d). Fluorescent nuclei can be clearly seen within cells that have entered into the process of lignification, as the

characteristic rings of lignin can be seen as bands already surrounding this cell in Figure 4i.

Reporter lines marking developmental stages of the primary root

Cells in the primary root progress through a series of developmental identities, from stem cells to the transit amplifying cells of the meristem and the post-mitotic, but endo-replicating cells of the differentiation zone. The processes that control the progressive reduction of proliferation and the transition to differentiation are still not well understood, so lines marking these developmental transitions are likely to be of high utility. We aimed to generate such orthogonal markers to report in all tissue types at any one developmental stage (Table S2).

The AQC/TPST (At1g08030) promoter-driven stem cell line (V241) marks the stem cell niche and in most of the stem cells surrounding the stem cell niche (Figure 1b–e). However, expression in the vascular stem cells is variable, with 50% of the selected lines lacking expression in the vascular stem cells (Figure 1b,d). H2B-Venus fluorescence is also seen in the one–two immediate progeny of the columella and lateral root cap stem cells, but no expression is seen outside of this region within the root apical meristem.
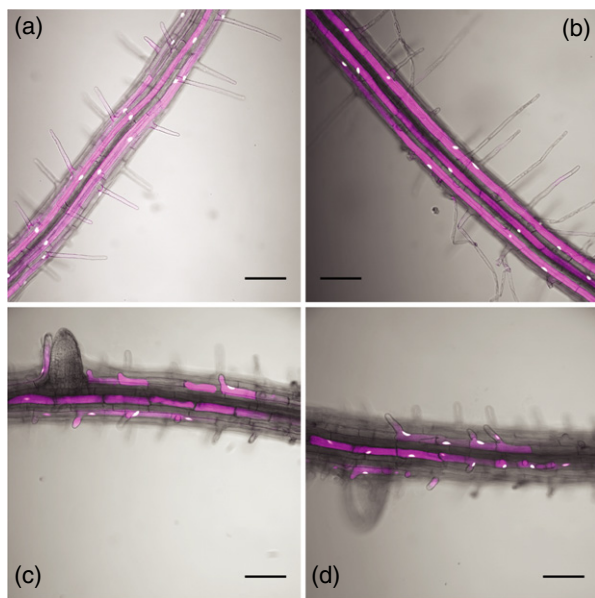
Figure 5. Production of Anthocyanin Pigment 1 (PAP1)-expressing lines demonstrate tissue-specificity of gene expression.
White indicates H2B-Venus fluorescence and magenta indicates fluorescence caused by anthocyanin accumulation.
(a and b) Mature root of V101 >> PAP1, with anthocyanin accumulating in the atrichoblast cells.
(c and d) Mature root of V111 >> PAP1, anthocyanin accumulates in the trichoblast cells. Scale bar: 100 μm.

The V311 line uses the promoter from TCP7 (At5g23280) that marks all tissues in the mature root, outside of the meristem (Figure S14a,b). The expression is not correlated with an increase in ploidy, as it is also expressed in the pericycle layer (Figure S14b,c), in which the cells do not endoreplicate (Beeckman *et al.*, 2001).

Several lines were constructed to generate a line specific to the root apical meristem or the root apical meristem and transition domain, including DEL1 (At3g48160), APC11 (At3g05871). However, we failed to identify a line that satisfied the requirement to be specific to the meristem: fluorescent protein accumulation was observed in the differentiation zone of the root. In addition, several promoter sequences were tested for the development of a stem cell niche-specific reporter line, including QC46 (ten Hove *et al.*, 2010) and mAGL42 (Nawy *et al.*, 2005), but none was found to result in expression that was specific to the QC cells beyond 4 days after germination (d.a.g.).

Reporter lines as tissue-specific drivers of secondary gene expression

One or more additional Effector plasmid constructs containing a gene expressed under control of the LexAop sequence can be introduced into a Driver line, resulting in tissue-specific, estradiol-inducible gene expression. Effector constructs may be inserted into Driver lines by crossing, as was done with the diphtheria toxin chain A (DTA)

Effector line, or by direct transformation as was done with the PAP1 effector line (Figure 5a–d).

The p35S line (C01) uses H2B-mCherry as a fluorescent reporter, and fluorescence is observed in every cell in the plant, including the root apical meristem (Figure S15a,b). DTA functions as an extremely potent, cell-autonomous ADP-ribosylase of the EF2 translation initiation factor, and consequently inhibits all protein translation, eventually leading to cell death (Collier, 1975; Pappenheimer, 1977; Yamaizumi *et al.*, 1978). Controlled delivery of DTA to ablate cells has been successfully used in plants for studies of pistil and anther development, lateral root development, regeneration and root cap sensing (Tsugeki and Fedoroff, 1999; Laplaze *et al.*, 2005; Che *et al.*, 2007). We used DTA to evaluate the tightness of regulation of activation of the XVE system.

C01 was crossed with the DTA Effector line (see Figure S16 for map of construct) containing the LexAop-DTA plasmid construct. F3 progeny were selected on hygromycin and kanamycin for the presence of at least one copy of the Driver (C01) and Effector (DTA) construct and transferred to 0.5 × MS plates with 5 μM estradiol. All seedlings were bleached 7 days after transfer (Figure S17). Without estradiol, however, all plants grow to maturity after transplanting to soil with no observed growth defects, demonstrating that DTA is not being expressed and revealing the robust control of the estradiol induction in this system (Figure S17).

Diphtheria toxin A expression was also shown to function in a tissue-specific manner by crossing the LexA:DTA construct into V101 to produce estradiol-inducible DTA expression specific to the atrichoblast cells of the epidermis (Figure S19). Propidium iodide is used here as a live/dead stain so that cells with damaged membranes are heavily stained with propidium iodide. The cell death is restricted to the atrichoblast file of the epidermis and does not appear to cause damage to the other tissue layers of the root. This cell death phenotype was not clearly highlighted by propidium iodide in the root apical meristem, but the absence of H2B-Venus expression in the meristem suggests the onset of DTA-dependent translation inhibition.

To demonstrate the tissue-specificity of secondary gene expression, we used a vital reporter of activity. Production of Anthocyanin Pigment 1 (PAP1; At1g56650) is a master regulator for anthocyanin production and, when overexpressed, it can produce visible anthocyanin staining (Borevitz *et al.*, 2000). The accumulating anthocyanins are visible by both fluorescence (Poustka *et al.*, 2007) and brightfield microscopy, and thus PAP1 can also function as a new genetically encoded visible reporter gene. The PAP1 plasmid construct was transformed directly into the homozygous Driver lines of V101, the atrichoblast marker line, and V111, the trichoblast marker line, and the

resulting transformed plants were screened by brightfield microscopy for visible pink colouration after estradiol induction. We deliberately screened for visible anthocyanin expression to identify high-level anthocyanin accumulation. Hence, we likely missed many low-expressing lines, as the sensitivity for brightfield detection of anthocyanins in this system is significantly lower than when detecting by fluorescence. For the transformation of V101, we analysed 42 independent transformants, of which 29 segregated 3:1, of which seven showed the expected, correct pattern of high-level expression, and none showed an unexpected pattern of expression. For the transformation of V111_25D, we analysed 42 independent transformants, of which 35 segregated 3:1, of which two showed the expected pattern of high-level expression, and none showed an unexpected pattern of expression. V101 >> PAP1 and V111 >> PAP1 demonstrates the tissue-specificity of the Effector gene expression system (Figure 5a–d): anthocyanin fluorescence is exclusively localised to the cells with yellow fluorescent nuclei.

DISCUSSION

We developed and functionally tested a versatile system for quantitatively, spatially and temporally controlling inducible gene expression in Arabidopsis. All reagents are available from the Arabidopsis Stock Centre to provide the basis for a well-characterised community resource that can be further expanded (Table S2). Promoter activity is visualised by the accumulation of nuclear-localised fluorescent proteins. This system was used to generate and characterise plant lines with expression directed to all major cell types of the root and three developmental domains of the root: the distal meristem (V431; lateral root cap, columella; Figure 2s–u); the stem cell niche and stem cells (G240, V241, K242, C243; Figure 1b–e); and differentiating cells (V311, expanding and differentiating cells; Figure S14). Experiments with DTA revealed very tight regulation of dependant protein accumulation after addition of estradiol to the specifically expressed synthetic transcription factor XVE (Figure S17). Silencing of constructs was not observed over four–five generations. These results validate the utility and specificity of the system to provide an expandable community-wide resource for more reproducible and comparable data generation.

Design principles

We implemented several design principles to allow these lines to be shared with and efficiently used by other researchers. First, we embedded a nuclear-localised reporter that indicates activation by estradiol of the XVE transcription factor expressed under control of the desired promoter (Figure S1) in *cis*, which together comprise the Driver construct. This will facilitate crosses of the Driver into the desired mutant or transgenic backgrounds.

Second, all constructs were transformed into Col-0, as this is the most commonly used genetic background in Arabidopsis research, again to facilitate their use alongside existing mutants and transformed lines. As the XVE vectors and promoter-XVE constructs are available, new lines can be generated in any desired accession or other species to expand the utility of the system for the community further. Third, there are four alternative plasmids for Driver constructs, each made with a different fluorescent protein (GFP, Venus, monomeric Kusabira Orange and monomeric Cherry). The variety of different fluorescent protein reporters enables the lines to be used alongside existing fluorescent reporter lines by selecting a complementary fluorescent protein that can be spectrally resolved from the pre-existing reporter in the desired plant background. Lastly, the decision was made to use nuclear-localised fluorescent proteins. This gives more clarity than cytosolic fluorescence when determining expression domains by microscopy, especially at low expression levels, and improves quantification of fluorescence from fluorescence image data.

Characterisation of expression patterns

Reporter constructs introduced into Arabidopsis by Agrobacterium-mediated transformation insert at semi-random positions, which can influence the pattern and magnitude of fluorescent reporter activity of individual transformation events (Peach and Velten, 1991; Schubert *et al.*, 2004; Marques-Bueno *et al.*, 2016). To enhance the utility of the reporter lines and promote efforts to increase reproducibility across different laboratories, we extensively characterised and documented the expression patterns in the lines we share as a resource with the community to provide a degree of experimental standardisation. We observed differences in accumulation of nuclear localised fluorescent reporters, with respect to intensity and pattern after standardised estradiol induction treatments between independently transformed lines. This, to a minor extent, reflected in the subtle variations observed in the different lines transformed with AQC1 promoter-directed expression of GFP, Venus, mKO and mCherry, respectively (Figure 1). Such variation reinforces the need to utilise well-characterised and shared Driver lines across the community to enhance reproducibility. The community-wide use of such well-defined reference resources has recently been facilitated by the optimisation of CRISPR/Cas9-based methods, which make it easier to regenerate desired single or multiple hypomorphic alleles in such a standard reporter line than to introgress such alleles over several generations (Ordon *et al.*, 2017).

Expression patterns of genes change throughout the development of an organism, and so only one developmental stage (7–12 d.a.g.) was used for the characterisation of the lines. While characterisation of expression patterns

in very young (3–5 d.a.g.) seedlings is relatively common in the literature, we observed that these seedlings do not reflect the gene expression patterns of fully photoautotrophic, environmentally responsive plants. For example, although we observed fluorescent protein expression in several independent lines that had been transformed with the QC46 (ten Hove *et al.*, 2010) and mAGL42 (Nawy *et al.*, 2005) promoters directing XVE expression at 3–5 d.a.g., by 7 d.a.g. this had been lost. Therefore, the characterisation of expression patterns of the reporter lines focused only on primary roots at 7–12 d.a.g. to indicate expression behaviour in photoautotrophic seedlings.

Fusion of H2B fragments with fluorescent proteins can have a stabilising effect that can broaden the expression domain. In the lines presented here, however, the expression domains appear identical to those in the studies from which the promoter sequences were taken. The V251 line driving expression in the meristem cortex cells (CO2 promoter) shows a rapid extinguishing of fluorescence that is consistent with the predicted pattern of meristem cortex cells.

Advantages of the new XVE system

Fluorescent reporter lines that mark individual tissues have been developed previously, initially the enhancer trap lines developed by the Haseloff (Haseloff, 1999; Laplaze *et al.*, 2005) and the promoter trap lines developed by the Pelletier (Bechtold *et al.*, 1993) groups, which were generated in the C24 or Wassilevskija (Ws) accessions, respectively, which are currently not widely used for molecular-genetic work. By contrast, we generated lines in the broadly used Col-0 accession. Moreover, the lines presented here are fully characterised in terms of expression pattern in order to facilitate use by other researchers, and we encourage other users to add to the collection by making their lines public.

A distinct advantage of the XVE system is its rapid inducibility and good dose–responsivity (Zuo *et al.*, 2000, this work): we examined a time course of induction and observed half-maximal induction between 3 and 6 h, and a good range of dose–responsivity after 24 h (Figure S18).

There remains a distinct lack of available reporter lines and characterised promoters that are specific for different developmental stages in the Arabidopsis root and that are in the same genetic background. The Arabidopsis root is composed of tissues that have markedly different properties, including proliferation rate, ploidy and vacuolation, so it is highly desirable to be able to label, separate and drive ectopic expression in these tissues very specifically and accurately. Previously, this functionality has been approximated by microdissection, as seen in reports by Birnbaum, Brady and colleagues (Birnbaum *et al.*, 2003; Brady *et al.*, 2007), but this is tedious and lacks the accuracy and reproducibility of a well-characterised reporter line.

Effector gene constructs can be added into driver lines by either direct transformation or by crossing. Both methods require the same number of generations to produce experimental lines that are homozygous for both constructs, but preliminary characterisation can occur earlier in transformed lines due to the semi-dominant nature of the XVE transcription factor. It should be noted that the transformation of the secondary plasmids will also result in variations in insertion, which will result in variations in expression level. This system still maintains the distinct advantage of an unchanging expression domain, so that only the level and not the spatial pattern of secondary gene expression needs to be measured when selecting lines.

PAP1 as a new vital reporter

PAP1 has been previously used to effect anthocyanin accumulation in shoot tissues (Borevitz *et al.*, 2000). We examined here the utility of PAP1 in controlling anthocyanin accumulation in specific root cell types with a view to generate a cell-autonomous, encoded effector to mediate stable marking of cells. Anthocyanin accumulated specifically in cells in which PAP1 was expressed, although it took several days for strong visible pigmentation to develop. We used the wild-type coding sequence for PAP1, but as PAP1 requires phosphorylation for stability and full activity, anthocyanin accumulation could be accelerated by use of phospho-mimic mutations (Li *et al.*, 2016).

In conclusion, we have generated a modular, validated and expandable system to direct gene expression in many tissues and cell types of the Arabidopsis root with utility for developmental, physiological and cellular studies. These lines have been donated to the Nottingham Arabidopsis Stock Centre (Table S2).

EXPERIMENTAL PROCEDURES

Generation and cloning of vectors and promoter sequences

Generation of vectors is described in Supplemental Methods. Promoter sequences were amplified using the primers listed in Table S1, Arabidopsis Col-0 genomic DNA and Q5 (NEB) enzyme using the manufacturer's recommended conditions.

Seedling sterilisation and growth for microscopy

Arabidopsis seeds were placed in either 1.5-ml Eppendorf tubes or 15-ml Falcon tubes. Seeds were washed with a solution of 70% ethanol with 0.05% Tween for 15 min with shaking, which was then replaced with a solution of 95% ethanol for 3 min. The ethanol solution and the seeds were placed on a sterile filter paper in a laminar flow hood until dry. Seedlings for microscopy were sterilised as above, and sown on 12-cm^2 plates containing 50 ml of $0.5 \times$ MS salts, 1% sucrose, with pH adjusted to 5.8 using KOH and solidified with 1% agar. Media was supplemented with 5 μM estradiol from a stock of 100 mM estradiol in ethanol. Two rows of 10 seeds were sown on each plate. The plates were stratified at 4°C for 2 days, and then transferred to a growth room where they were placed vertically for 7–10 days.

Estradiol induction for diphtheria toxin A

Twenty-five F2 seeds from the cross of 35S:XVE>H2B-mCherry and 35S:XVE>> LexAop:DTA were each sown onto 9-cm Petri dishes containing 25 ml of $0.5 \times$ MS salts, 0.6% sucrose and solidified with 1% agar. pH was adjusted to 5.8 with KOH. The seeds were stratified for 2 days and then placed in a growth chamber. At 7 days, the plates were flooded with 20 ml of $0.5 \times$ MS salts, 0.6% sucrose, and either 5 μM estradiol or a control of vehicle only. Five days post-induction, the plates were photographed using a digital camera and a lightbox.

Confocal microscopy

Slides were prepared by placing primary roots onto the slide in a solution of $0.5 \times$ MS containing 5 μg ml^{-1} propidium iodide. Slides were used immediately for microscopy. An Olympus confocal FV300 on an IX70 inverted microscope with an Argon laser and a Helium-Neon laser (Ex, 488 nm, 543 nm, respectively) was used for all confocal imaging. Images were taken using either a 20 ×, 40 × or 60 × water immersion lens.

H2B-eGFP/Venus and propidium iodide fluorescence were visualised using both 488 nm and 543 nm excitation, a 510-nm long-pass filter (BA510IF), a 530-nm short-pass filter (BA530RIF) and a 585/640-nm band-pass filter (BA585-640). mKO fluorescence was visualised using 543-nm excitation and a 585/640-nm band-pass filter (BA585-640). mCherry fluorescence was visualised using 543-nm excitation and a 585/640-nm band-pass filter (BA585-640). The transmitted light channel was used to provide a spatial reference. Venus and anthocyanin fluorescence were visualised using both 488-nm and 543-nm excitation, a 510-nm long-pass filter (BA510IF), a 530-nm short-pass filter (BA530RIF) and a 585/640-nm band-pass filter (BA585-640), as described (Poustka *et al.*, 2007). The transmitted light channel was used to provide a spatial reference.

Images were converted to single-channel RGB colour images using FIJI. Digital cross-sections were made in FIJI, using Z-stacks generated with 3-μm intervals.

Dye loading of carboxytetraethylrhodamine

Carboxytetraethylrhodamine (CTER; CAS, 37299-86-8; Acros; Knoblauch *et al.*, 2015) was loaded into the cotyledons of seedlings 30 min prior to the start of microscopy. CTER was loaded as follows, cotyledons were first gently damaged by compression with a pair of ridged forceps, and then 1 μl of 0.8 mM CTER solution was added to the wounded cotyledon. Seedlings were kept in a closed Petri dish for 30 min to maintain a humid environment, and then seedlings were imaged by confocal microscopy.

AUTHOR CONTRIBUTIONS

XT and PD performed cloning of promoters and vectors; FQM and MB performed confocal imaging; FQM performed DTA experiments. MB, AF and TC performed confocal imaging of anthocyanin fluorescence. FQM and PD wrote the paper. W-RS provided space and resources to PD during part of this work.

SUPPORTING INFORMATION

Additional Supporting Information may be found in the online version of this article.

Figure S1. Map of pXVG vector.

Figure S2. Maps of XVE>H2B-FP vector series.

Figure S3. Images of pGL2 > H2B-Venus (**V101**_15B).

Figure S4. Images of pSHV2 > H2B-Venus (**V111**_25D).

Figure S5. Images of pCO$_2$ > H2B-Venus (**V251**_6G).

Figure S6. Images of pE49 > H2B-Venus (**V121**_6B).

Figure S7. Images of pSCR>H2B-Venus (**V141**_21E).

Figure S8. Images of pDAG1 > H2B-Venus (**V181**_23D).

Figure S9. Images of At5g09760 > H2B-Venus (**V151**_27A).

Figure S10. Images of pAt2g18380 > H2B-Venus (**V201**_18A).

Figure S11. Images of pAt2g18380 > H2B-Venus (**V201**_18A) and pAt3g25710 > H2B-Venus (**V261**_1F).

Figure S12. Images of pSUC2 > H2B-eGFP (**G235**_32A).

Figure S13. Images of pAt3g25710 > H2B-Venus (**V261**_1F).

Figure S14. Images of pTCP7 > H2B-Venus (**V311**_1N).

Figure S15. Images of p35S > H2B-mCHERRY (**C01**_17B).

Figure S16. Map of the DT-A gene in the pMDC221 vector.

Figure S17. Images of the progeny of the cross of C01 (Driver) and DTA in pMDC221 (Effector).

Figure S18. Time course and dose–response of estradiol induction.

Figure S19. Tissue-specific cell ablation in V101 >> DTA.

Supplemental Methods. Construction of pXVE-FP vectors.

Table S1. Primers used for promoter amplification

Table S2. List of lines donated to Stock Centre

REFERENCES

Bechtold, N., Ellis, J. and Pelletier, G. (1993) *In planta* Agrobacterium-mediated gene transfer by infiltration of adult *Arabidopsis thaliana* plants. *C. R. Acad. Sci. Paris, Life Sci.* **316**, 1194–1199.

Beeckman, T., Burssens, S. and Inze, D. (2001) The peri-cell-cycle in Arabidopsis. *J. Exp. Bot.* **52**, 403–411.

Birnbaum, K., Shasha, D.E., Wang, J.Y., Jung, J.W., Lambert, G.M., Galbraith, D.W. and Benfey, P.N. (2003) A gene expression map of the Arabidopsis root. *Science* **302**, 1956–1960.

Borevitz, J.O., Xia, Y., Blount, J., Dixon, R.A. and Lamb, C. (2000) Activation tagging identifies a conserved MYB regulator of phenylpropanoid biosynthesis. *Plant Cell* **12**, 2383–2394.

Brady, S.M., Orlando, D.A., Lee, J.Y., Wang, J.Y., Koch, J., Dinneny, J.R., Mace, D., Ohler, U. and Benfey, P.N. (2007) A high-resolution root spatiotemporal map reveals dominant expression patterns. *Science* **318**, 801–806.

Brand, L., Horler, M., Nuesch, E., Vassalli, S., Barrell, P., Yang, W., Jefferson, R.A., Grossniklaus, U. and Curtis, M.D. (2006) A versatile and reliable two-component system for tissue-specific gene induction in Arabidopsis. *Plant Physiol.* **141**, 1194–1204.

Charlton, W.A. (1991) Lateral root initiation. In *Plant Roots: The Hidden Half* (Weisel, Y., Eshel, A. and Kafkafi, U., eds). New York: M. Dekker.

Che, P., Lall, S. and Howell, S.H. (2007) Developmental steps in acquiring competence for shoot development in Arabidopsis tissue culture. *Planta* **226**, 1183–1194.

Collier, R.J. (1975) Diphtheria toxin: mode of action and structure. *Bacteriol. Rev.* **39**, 54–85.

Esau, K. (1965) *Plant Anatomy*, 2d edn. New York: Wiley.

Goddijn, O.J., Lindsey, K., van der Lee, F.M., Klap, J.C. and Sijmons, P.C. (1993) Differential gene expression in nematode-induced feeding structures of transgenic plants harbouring promoter-gusA fusion constructs. *Plant J.* **4**, 863–873.

Haseloff, J. (1999) GFP variants for multispectral imaging of living cells. *Methods Cell Biol.* **58**, 139–151.

Heidstra, R., Welch, D. and Scheres, B. (2004) Mosaic analyses using marked activation and deletion clones dissect Arabidopsis SCARECROW action in asymmetric cell division. *Genes Dev.* **18**, 1964–1969.

Helariutta, Y., Fukaki, H., Wysocka-Diller, J., Nakajima, K., Jung, J., Sena, G., Hauser, M.T. and Benfey, P.N. (2000) The SHORT-ROOT gene controls radial patterning of the Arabidopsis root through radial signaling. *Cell* **101**, 555–567.

ten Hove, C.A., Willemsen, V., de Vries, W.J., van Dijken, A., Scheres, B. and Heidstra, R. (2010) SCHIZORIZA encodes a nuclear factor regulating asymmetry of stem cell divisions in the Arabidopsis root. *Curr. Biol.* **20**, 452–457.

Kang, H.G., Fang, Y. and Singh, K.B. (1999) A glucocorticoid-inducible transcription system causes severe growth defects in Arabidopsis and induces defense-related genes. *Plant J.* **20**, 127–133.

Kanno, S., Arrighi, J.F., Chiarenza, S. et al. (2016) A novel role for the root cap in phosphate uptake and homeostasis. *Elife* **5**, e14577.

Karasawa, S., Araki, T., Nagai, T., Mizuno, H. and Miyawaki, A. (2004) Cyanemitting and orange-emitting fluorescent proteins as a donor/acceptor pair for fluorescence resonance energy transfer. *Biochem. J.* **381**, 307–312.

Knoblauch, M., Vendrell, M., de Leau, E., Paterlini, A., Knox, K., Ross-Elliot, T., Reinders, A., Brockman, S.A., Ward, J. and Oparka, K. (2015) Multispectral phloem-mobile probes: properties and applications. *Plant Physiol.* **167**, 1211–1220.

Laplaze, L., Parizot, B., Baker, A., Ricaud, L., Martiniere, A., Auguy, F., Franche, C., Nussaume, L., Bogusz, D. and Haseloff, J. (2005) GAL4-GFP enhancer trap lines for genetic manipulation of lateral root development in *Arabidopsis thaliana*. *J. Exp. Bot.* **56**, 2433–2442.

Lee, J.Y., Colinas, J., Wang, J.Y., Mace, D., Ohler, U. and Benfey, P.N. (2006) Transcriptional and posttranscriptional regulation of transcription factor expression in Arabidopsis roots. *Proc. Natl Acad. Sci. USA* **103**, 6055–6060.

Li, S., Wang, W., Gao, J., Yin, K., Wang, R., Wang, C., Petersen, M., Mundy, J. and Qiu, J.L. (2016) MYB75 phosphorylation by MPK4 is required for light-induced anthocyanin accumulation in Arabidopsis. *Plant Cell* **28**, 2866–2883.

Marques-Bueno, M.D.M., Morao, A.K., Cayrel, A., Platre, M.P., Barberon, M., Caillieux, E., Colot, V., Jaillais, Y., Roudier, F. and Vert, G. (2016) A versatile multisite gateway-compatible promoter and transgenic line collection for cell type-specific functional genomics in Arabidopsis. *Plant J.* **85**, 320–333.

Nagai, T., Ibata, K., Park, E.S., Kubota, M., Mikoshiba, K. and Miyawaki, A. (2002) A variant of yellow fluorescent protein with fast and efficient maturation for cell-biological applications. *Nat. Biotechnol.* **20**, 87–90.

Nawy, T., Lee, J.Y., Colinas, J., Wang, J.Y., Thongrod, S.C., Malamy, J.E., Birnbaum, K. and Benfey, P.N. (2005) Transcriptional profile of the Arabidopsis root quiescent center. *Plant Cell* **17**, 1908–1925.

Ordon, J., Gantner, J., Kemna, J., Schwalgun, L., Reschke, M., Streubel, J., Boch, J. and Stuttmann, J. (2017) Generation of chromosomal deletions in dicotyledonous plants employing a user-friendly genome editing toolkit. *Plant J.* **89**, 155–168.

Pappenheimer, A.M. Jr (1977) Diphtheria toxin. *Annu. Rev. Biochem.* **46**, 69–94.

Parizot, B., Laplaze, L., Ricaud, L. et al. (2008) Diarch symmetry of the vascular bundle in Arabidopsis root encompasses the pericycle and is reflected in distich lateral root initiation. *Plant Physiol.* **146**, 140–148.

Peach, C. and Velten, J. (1991) Transgene expression variability (position effect) of CAT and GUS reporter genes driven by linked divergent T-DNA promoters. *Plant Mol. Biol.* **17**, 49–60.

Poustka, F., Irani, N.G., Feller, A., Lu, Y., Pourcel, L., Frame, K. and Grotewold, E. (2007) A trafficking pathway for anthocyanins overlaps with the endoplasmic reticulum-to-vacuole protein-sorting route in Arabidopsis and contributes to the formation of vacuolar inclusions. *Plant Physiol.* **145**, 1323–1335.

Pyo, H., Demura, T. and Fukuda, H. (2004) Spatial and temporal tracing of vessel differentiation in young Arabidopsis seedlings by the expression of an immature tracheary element-specific promoter. *Plant Cell Physiol.* **45**, 1529–1536.

Ross-Elliott, T.J., Jensen, K.H., Haaning, K.S. et al. (2017) Phloem unloading in Arabidopsis roots is convective and regulated by the phloem-pole pericycle. *Elife* **6**, e24125 https://doi.org/10.7554/eLife.24125.

Schubert, D., Lechtenberg, B., Forsbach, A., Gils, M., Bahadur, S. and Schmidt, R. (2004) Silencing in Arabidopsis T-DNA transformants: the predominant role of a gene-specific RNA sensing mechanism versus position effects. *Plant Cell* **16**, 2561–2572.

Schurholz, A.K., Lopez-Salmeron, V., Li, Z. et al. (2018) A comprehensive toolkit for inducible, cell type-specific gene expression in arabidopsis. *Plant Physiol.* **178**, 40–53.

Shaner, N.C., Campbell, R.E., Steinbach, P.A., Giepmans, B.N., Palmer, A.E. and Tsien, R.Y. (2004) Improved monomeric red, orange and yellow fluorescent proteins derived from *Discosoma* sp. red fluorescent protein. *Nat. Biotechnol.* **22**, 1567–1572.

Siligato, R., Wang, X., Yadav, S.R. et al. (2016) MultiSite gateway-compatible cell type-specific gene-inducible system for plants. *Plant Physiol.* **170**, 627–641.

Steeves, T.A. and Sussex, I.M. (1989) *Patterns in Plant Development*, 2nd edn. Cambridge: Press Syndicate of the University of Cambridge.

Su, S.H., Gibbs, N.M., Jancewicz, A.L. and Masson, P.H. (2017) Molecular mechanisms of root gravitropism. *Curr. Biol.* **27**, R964–R972.

van Tieghem, P. and Douliot, H. (1888) Recherches comparatives sur l'origine des membres endogènes. *Ann. Sci. Natur. Bot. 7e sér* **8**, 1–660.

Tsien, R.Y. (1998) The green fluorescent protein. *Annu. Rev. Biochem.* **67**, 509–544.

Tsugeki, R. and Fedoroff, N.V. (1999) Genetic ablation of root cap cells in Arabidopsis. *Proc. Natl Acad. Sci. USA* **96**, 12 941–12 946.

Xiao, Y.L., Redman, J.C., Monaghan, E.L., Zhuang, J., Underwood, B.A., Moskal, W.A., Wang, W., Wu, H.C. and Town, C.D. (2010) High throughput generation of promoter reporter (GFP) transgenic lines of low expressing genes in Arabidopsis and analysis of their expression patterns. *Plant Methods* **6**, 18.

Yamaguchi, M., Kubo, M., Fukuda, H. and Demura, T. (2008) Vascular-related NAC-DOMAIN7 is involved in the differentiation of all types of xylem vessels in Arabidopsis roots and shoots. *Plant J.* **55**, 652–664.

Yamaizumi, M., Mekada, E., Uchida, T. and Okada, Y. (1978) One molecule of diphtheria toxin fragment A introduced into a cell can kill the cell. *Cell* **15**, 245–250.

Zhou, W., Wei, L., Xu, J. et al. (2010) Arabidopsis Tyrosylprotein sulfotransferase acts in the auxin/PLETHORA pathway in regulating postembryonic maintenance of the root stem cell niche. *Plant Cell* **22**, 3692–3709.

Zuo, J., Niu, Q.W. and Chua, N.H. (2000) Technical advance: An estrogen receptor-based transactivator XVE mediates highly inducible gene expression in transgenic plants. *Plant J.* **24**, 265–273.